Two-phase modeling of wall and bulk condensation by hybrid VOF-mixture approach for containment applications

Allen George[1,2]**, Stephan Kelm**[1]**, and Xu Cheng**[2]
[1]Institute of Energy and Climate Research, Forschungszentrum Jülich GmbH, Jülich, Germany
[2]Institute for Applied Thermofluidics (IATF), Karlsruhe Institute of Technology Karlsruhe, Germany
a.george@fz-juelich.de; s.kelm@fz-juelich.de; xu.cheng@kit.edu

ABSTRACT

Condensation (wall and bulk) in the presence of non-condensable gases is a safety relevant phenomenon in nuclear reactors during a severe accident scenario like Loss of Coolant Accident (LOCA). An initial single-phase approach revealed the need to also consider the accumulation of condensate in sumps. Thus, the present work models condensation processes inside a containment using a hybrid volume-of-fluid (VOF) and mixture approach with continuous gas phase consisting of steam-air mixture, and water phase constituting both dispersed fog droplets and continuous water. The dispersed fog droplets can drift relative to the continuous gas phase by the effects of gravity, inertia, drag and diffusion. The differentiation between the continuous and dispersed phases and corresponding model selections are facilitated using a blending function based on the phase volume fraction. Contrary to the traditional VOF or mixture method of a single energy equation, separate energy equations are used for each phase to promote thermal non-equilibrium condition analysis. The wall condensation uses a diffusion layer model approach which is extended to handle interface film condensation on free surfaces. The bulk (or volume) condensation uses the saturation condition approach of bringing the local gas mixture to saturation temperature at constant timescale. The model solver is developed in OpenFOAM framework based on the 'compressibleInterFoam' solver and then added to containmentFOAM CFD package. The capability of the hybrid solver in capturing specific features of VOF and mixture models were initially verified using a dam break and bent pipe deposition cases. The bulk condensation model was verified on air-steam mixing (hot and cold) nozzle simulation which gave good agreement for fog quantity and mixture temperature w.r.t. Mollier diagram theory. The wall condensation model was validated using SETCOM (Forschungszentrum Jülich) and COPAIN experimental facility which predicted the wall heat flux with 95% accuracy. Finally, a multi-phenomena interaction experiment (THAI TH2, Becker Technologies Germany) was simulated which predicted the vessel conditions with reasonable accuracy.

KEYWORDS
VOF, mixture model, bulk condensation, wall condensation, fog, containmentFOAM

1. INTRODUCTION

Condensation of steam in a water-cooled nuclear reactor containment in the event of an accident is an important phenomenon that characterizes the reactor passive safety systems. In the course of a Loss of Coolant Accident (LOCA), steam and hydrogen are released into the reactor containment air atmosphere , thereby elevating the internal pressure and temperature. The steam condenses in the bulk forming fog droplets and on the containment walls and internal components in the form of films, droplets or rivulets. This results in reduction of pressure and also affects the local composition of steam-air-hydrogen mixture inside the containment. Also, some of these droplets and films may get transported to dry regions where they re-evaporate and contribute to pressure rise. Hence, it is necessary to model condensation and evaporation processes inside a reactor containment to predict the local conditions and locate regions of possible hydrogen combustion.

Previous condensation modelling investigations by Vyskocil et al. [1] used a single-phase method to study the effects of bulk and wall condensation in CONAN and PANDA experiments. Phase change was modelled using a mass sink approach which removed the condensate from the computational system and hence, transport and re-evaporation of water droplets and films were neglected. George et al. [2] extended this model by using an Eulerian passive scalar approach for fog transport and made re-evaporation of the water droplets also possible. However, the transport of wall condensate films and accumulation of water in the sump regions of experiments like THAI were impossible with passive scalar method. Zhang and Laurien [3] introduced two-fluid method consisting of a continuous gas phase and dispersed liquid phase to simulate volume condensation in a THAI experiment. Mimouni et al. [4] also used the two-fluid method to model wall condensation and evaporation and validated it on COPAIN and TOSQAN ISP47 experiments. The two-fluid model requires additional sub-models for closure and involves two sets of conservation equations which might be sumptuous for containment applications.

This paper introduces the Volume of Fluid (VOF) approach combined with mixture model to predict bulk and wall condensation as well as transport and accumulation of the condensate in a containment. This method uses the mixture approach in regions where the water phase is in dispersed form and VOF approach in continuous regions, and a blending function helps to smoothen this transition. Since this method uses mixture conservation equations, they are relatively cheaper computationally compared to the two-fluid method. However, this approach restricts the model capability to capture relative motion of dispersed droplets and thermal non-equilibrium between the phases. These limitations are resolved in the present work by incorporating drift flux approach to the mixture method to model droplet slip velocity and also by using separate energy equations for each phase. The wall condensation is modelled using diffusion layer approach and modified to simulate interface condensation and bulk condensation is based on bringing the local mixture to saturation temperature to model formation of fog. The solver is developed in OpenFOAM based CFD package, *containmentFOAM* [5] CFD package to model containment thermal hydraulics. The hybrid approach was initially verified on a dam break and bent pipe deposition cases to ensure that the main characteristics of VOF and mixture model were captured.The model validation studies for wall condensation were performed on COPAIN and SETCOM experiments, and bulk condensation model was verified using Mollier theory. Additionally, the model was tested on a technical scale THAI TH2 experiment where both wall and bulk condensation are important. For all the validation studies, the solver was able to predict the experimental data with reasonable accuracy. Moreover, the two-phase model was effective in capturing extra features like accumulation of water in sump region and thermal non-equilibrium between phases, which were not possible with a single-phase solver.

2. MODELLING APPROACH

The solver uses a hybrid VOF - Mixture method with drift flux (or algebraic slip) approach to model containment thermal hydraulics. The first phase is water which can be in the form of either dispersed droplets (fog) or continuous phase (water). The second phase is a multi-species gas mixture which composes of steam and non-condensable gases like air, helium or hydrogen. The mixture model allows the phases to be interpenetrating and have relative velocities which is used in fog regions whereas the VOF model is designed for immiscible fluids and can track phase interfaces which are used in continuous water regions. The OpenFOAM solver ‘compressibleInterFoam‘ is used as the base solver for development of the model code. A major assumption in the current model is that fog diameter is constant during a simulation and droplet evolution due to coalescence or breakup is neglected. A droplet diameter dependency study was performed on relevant cases to understand its effect on the results.

2.1. Governing Equations

The mathematical model is composed of a set of conservation equations for mass, momentum, and energy. The physical properties of the mixture like density and viscosity are defined as phase volume fraction weighted average of the corresponding phase properties.

Mixture mass continuity equation: The continuity equation for the mixture is defined in terms of the mixture density ρ and mixture velocity which is applicable to both VOF and mixture methods.

$$\frac{\partial \rho}{\partial t} + \nabla \cdot \left(\rho \vec{U}\right) = 0 \tag{1}$$

Phase mass balance equations: For the system of gas and water phases, the phase mass conservation equation is defined in terms of the phase volume fractions (α_1 and α_2) with additional mass transfer term ($\dot{m}'''$) which handles mass exchange between the two phases due to condensation or evaporation.

$$\frac{\partial \alpha_1 \rho_1}{\partial t} + \nabla \cdot \left(\alpha_1 \rho_1 \vec{U}\right) = \dot{m}''' \tag{2}$$

$$\frac{\partial \alpha_2 \rho_2}{\partial t} + \nabla \cdot \left(\alpha_2 \rho_2 \vec{U}\right) = -\dot{m}''' \tag{3}$$

Here, α_1 is the volume fraction of water (fog) and α_2 is the volume fraction of gas mixture. The variables ρ_1 and ρ_2 represents the mass densities of the corresponding phases. Also, the sign convention for the mass transfer term is that $\dot{m}'''$ is positive for condensation and negative for evaporation. This equation is common for VOF as well as mixture methods if relative velocity is neglected.

Considering both phases to be compressible and combining eqns. 2 and 3, we get the phase volume fraction transport equation as follows:

$$\frac{\partial \alpha_1}{\partial t} + \nabla \cdot \left(\alpha_1 \vec{U}\right) = \alpha_1 \nabla \cdot \vec{U} + \alpha_1 \alpha_2 \left[\frac{1}{\rho_2}\frac{D\rho_2}{Dt} - \frac{1}{\rho_1}\frac{D\rho_1}{Dt}\right] + \dot{m}''' \left[\frac{1}{\rho_1} - \alpha_1 \left(\frac{1}{\rho_1} - \frac{1}{\rho_2}\right)\right] \tag{4}$$

The above equation is applicable only when the first phase is in continuous form. When the water phase is in the form of dispersed fog droplets, they can drift relative to the mixture by the effects of gravity, inertia, and diffusion (turbulent and Brownian diffusion) and eqn. 4 is modified to include these phenomena as:

$$\begin{aligned}\frac{\partial \alpha_1}{\partial t} + \nabla \cdot \left(\alpha_1 \left(\vec{U} + \vec{u}_{drift}\right)\right) = \alpha_1 \nabla \cdot \vec{U} + \alpha_1 \alpha_2 \left[\frac{1}{\rho_2}\frac{D\rho_2}{Dt} - \frac{1}{\rho_1}\frac{D\rho_1}{Dt}\right] \\ + \nabla \cdot \left(\left(D_B + \nu_{t_2}/Sc_t\right) \nabla \alpha_1\right) + \dot{m}''' \left[\frac{1}{\rho_1} - \alpha_1 \left(\frac{1}{\rho_1} - \frac{1}{\rho_2}\right)\right]\end{aligned} \tag{5}$$

where D_B is the Brownian diffusion coefficient, ν_{t_2} is the turbulent viscosity of the gas phase and Sc_t is the turbulent Schmidt number

A blending function f_{α_1} is defined based on Mimouni et al. [4] to differentiate between dispersed and continuous phase and to smoothen this transition at a critical volume fraction (α_{crit}).

$$f_{\alpha_1} = \begin{cases} 1 - \frac{exp(-20(\alpha_1 - \alpha_{crit}))}{2} & \text{if } \alpha_1 > \alpha_{crit} \\ \frac{1}{2}\left(\frac{\alpha_1}{\alpha_{crit}}\right)^{20\alpha_{crit}} & \text{if } \alpha_1 \leq \alpha_{crit} \end{cases} \quad \text{where } \alpha_{crit} = 0.2 \tag{6}$$

This function is used to gradually change the mixture volume fraction equation (eqn. 5) to VOF volume fraction equation (eqn. 4) by multiplying the drift velocity and diffusion terms in eqn. 5 by $(1 - f_{\alpha_1})$. This blending function is also considered for modelling surface tension force, interface compression and inter-phase heat transfer.

Brownian diffusion is calculated by using Stokes- Einstein model [6, 7] where diffusion coefficient is a function of droplet diameter (d). The droplet drift velocity can be computed using the either by solving the Stokes model [8] force balance equation PDE iteratively or by a simplified Manninen model [7, 8] equation for droplet based on local equilibrium assumption that the acceleration of the droplet is equal to the acceleration of the mixture. The equations of the Stokes model drift velocity can be found in George et al. [2] and the Manninen model is shown below.

$$\vec{u}_{drift} = \frac{\rho_2 d^2}{18\mu_2}\left(\frac{\rho_1 - \rho_2}{\rho_1}\vec{g} - \frac{\partial \vec{U}}{\partial t}\right) \tag{7}$$

Here μ_2 is the dynamic viscoity of gas phase and $\vec{g}$ is the gravitational vector.

Specie transport equation:

The transport of each specie in the multi-component gas phase is modelled using the specie mass conservation equation where the mass transfer term ($\dot{m}_j'''$) is applicable only for condensable specie (steam).

$$\frac{\partial \alpha_2 \rho_2 Y_j}{\partial t} + \nabla \cdot (\alpha_2 \rho_2 \vec{U} Y_j) = \nabla \cdot \left[\alpha_2 \rho_2 \left(D_{j,m} + \frac{\nu_t}{Sc_t}\right)\nabla Y_j\right] + \dot{m}_j''' \tag{8}$$

Here, Y_j is the mass fraction of j-th species, $D_{j,m}$ is the molecular diffusivity of j-th specie in the gas mixture and m_j''' is the phase change mass source in j-th specie.

The diffusion coefficient of a specie in the mixture is computed from binary mass diffusion coefficients using Fick's law of diffusion.

$$D_{j,m} = \frac{1 - X_j}{\sum_{k \neq j} X_k / D_{jk}} \tag{9}$$

where D_{jk} is the binary diffusivity of phase pair $j - k$ and X_j is the molar fraction of the j-th specie.

Mixture momentum equation: The momentum equation of the VOF method which consists of surface tension force ($F_s = \sigma\kappa\nabla\alpha_1$) is combined with mixture method momentum equation which has additional term ($\tau_{drift} = \rho\frac{\alpha_1\rho_1}{\alpha_2\rho_2}\vec{u}^2_{drift}$) to include the effect of momentum diffusion due to relative motion of droplets [8], to

obtain the momentum conservation equation. Here also the blending function (f_{α_1}) helps in the transition of momentum equation from one method to another.

$$\frac{\partial \rho \vec{U}}{\partial t} + \nabla \cdot \left(\rho \vec{U} \otimes \vec{U} \right) + \nabla \cdot \tau_{drift} = -\nabla p + \nabla \cdot \tau + \rho \vec{g} + \sigma \kappa \nabla \alpha_1 \tag{10}$$

where τ is the viscous stress tensor, σ is the surface tension and κ is the interface curvature.

Phase energy transport equations:

The phase energy equations are described in terms of enthalpy and are solved for each phase to facilitate thermal non-equilibrium between phases. This approach is different from the traditional VOF or mixture method where we solve for a mixture energy equation. Here, we use transport equations similar to two-fluid model energy equations with a common mixture velocity field ($\vec{U}$) and the second phase (gas) has additional terms to include multi-component diffusion effects.

$$\frac{\partial \alpha_1 \rho_1 h_1}{\partial t} + \frac{\partial \alpha_1 \rho_1 K}{\partial t} + \nabla \cdot (\alpha_1 \rho_1 (\vec{U} + \vec{u}_{drift}) h_1) + \nabla \cdot (\alpha_1 \rho_1 (\vec{U} + \vec{u}_{drift}) K) = \alpha_1 \rho_1 \vec{U} \cdot \vec{g} + \alpha_1 \frac{\partial p}{\partial t} + \nabla \cdot (\lambda_{eff,1} \nabla T_1) + \kappa_1 (T_1 - T_2) + \dot{m}'''(h_1 + K) + \nabla H_{v1} \tag{11}$$

$$\frac{\partial \alpha_2 \rho_2 h_2}{\partial t} + \frac{\partial \alpha_2 \rho_2 K}{\partial t} + \nabla \cdot (\alpha_2 \rho_2 \vec{U} h_2) + \nabla \cdot (\alpha_2 \rho_2 \vec{U} K) = \alpha_2 \rho_2 \vec{U} \cdot \vec{g} + \alpha_2 \frac{\partial p}{\partial t} + \nabla \cdot (\lambda_{eff,2} \nabla T_2) + \sum_j \nabla \cdot \left[\alpha_2 \rho_2 h_{2,j} \left(D_{j,m} + \frac{\nu_t}{Sc_t} \right) \nabla Y_j \right] + \kappa_2 (T_2 - T_1) - \dot{m}'''(h_2 + K) + \nabla H_{v2} \tag{12}$$

where h_1 and h_2 are the phase specific enthalpies and K is the specific mixture kinetic energy. Here κ_1 and κ_2 are the inter-phase heat transfer coefficients and, $\lambda_{eff,1}$ and $\lambda_{eff,2}$ are the effective thermal conductivity of each phase. p is the mixture pressure and T_1 and T_2 are the temperature fields of each phase. The last term on the RHS of both equations includes the phase change effects on each phase energy equation. The latent heat released during condensation and absorbed during evaporation is equally distributed among two phases using the terms ∇H_{v1} and ∇H_{v2}.

Turbulence modelling:

For containment applications, the water phase accumulates in the sump regions and its velocities are low compared to the gas phase. Hence, it is reasonable to assume the water phase to be laminar, and turbulence equations are solved only for the gas phase to simplify the model. The coding implementation of a mixture turbulence model is not possible in the present OpenFOAM (v-9) framework as one of the phases is multi-component gas. The gas phase turbulence is modelled using standard $k - \omega$ SST model with additional buoyancy correction terms based on Simple Gradient Diffusion Hypothesis (SGDH) [9].

2.2. Wall and interface Condensation modelling

In the present work, wall condensation is modelled using diffusion layer method [10, 11] which is modified for two-phase flows and extended to simulate interface condensation. Wall condensation leads to the

formation of droplets which accumulate on the wall and then form a liquid film. During condensation, the steam will diffuse towards the wall or liquid-gas interface and non-condensable gases will accumulate in the vicinity due to its impermeability. Balancing the species mass fluxes due to diffusion and convective transport [10], the condensation mass flux across the wall or interface can be defined as:

$$\dot{m}''_{wall,interface} = \frac{\rho_2 D_{H_2O}}{1 - Y_{H_2O,sat}} \frac{Y_{H_2O} - Y_{H_2O,sat}}{\delta} \tag{13}$$

where ρ_2 is the density of the gas mixture and D_{H_2O} is diffusion coefficient of steam species in the gas mixture. Y_{H_2O} is the mass fraction of the steam at the cell center or at δ distance (computed from the mesh) from the wall or interface and $Y_{H_2O,sat}$ is the saturation mass fraction of steam on the wall or interface. The condensation mass flux is converted to volumetric mass transfer rate in near wall cell or near interface cell to add as a source (or sink) term to the continuity equation.

$$\dot{m}'''_{wall,interface} = \frac{A_{face}}{V_{cell}} \frac{\rho_2 D_{H_2O}}{1 - Y_{H_2O,sat}} \frac{Y_{H_2O} - Y_{H_2O,sat}}{\delta} \tag{14}$$

The A_{face} corresponds to the area of wall face for wall condensation and area of interface for interface condensation and V_{cell} is the volume of the cell. The transition from wall condensation to film (interface) condensation on the walls is done using the blending function f_{α_1}. The latent heat released during wall condensation is added to the wall directly (as boundary condition) for gas and droplet covered area and split between the water and gas phase in the film covered area. For interface condensation, the latent heat released is split between the water and gas phase.

2.3. Bulk Condensation modelling

The formation of fog by bulk (or volume) condensation is modelled by the "*return to saturation in a constant timescale*" method by Vyskocil et al. [1] which was previously used in a single-phase passive scalar solver by George et al. [2]. This model works by bringing the local mixture to a saturation state by condensing surplus steam or by evaporating the surplus fog. The amount of energy needed for heating (cooling) the local mixture to saturation temperature is released during condensation (evaporation) in numerical time step Δt.

$$Q = \alpha_2 \rho_2 C_{p_2} \frac{T_{sat}(p_{H_2O}) - T_2}{\Delta t} + \alpha_1 \rho_1 C_{p_1} \frac{T_{sat}(p_{H_2O}) - T_1}{\Delta t} \tag{15}$$

where C_{p_1} and C_{p_2} are the phase specific heat capacities and T_{sat} is the saturation temperature of the steam at partial pressure p_{H_2O}. The heat transfer term due to phase change (Q) is then divided by latent heat of vaporization to obtain bulk condensation rate.

$$\dot{m}'''_{bulk} = \frac{Q}{h_{fg}} \tag{16}$$

To prevent overlapping of bulk and wall condensation in the computational domain, the wall and interface condensation cells are initially marked, and the remaining cells are marked for bulk condensation. Also, the

condensation and evaporation rates are locally limited by the amount of steam and water present within a cell to conserve mass and energy.

3. RESULTS AND DISCUSSIONS

3.1. VOF and Mixture model validation

The VOF and mixture models are initially validated separately to show that the specific feature of each model is captured by the hybrid solver. To verify the phase transport, surface tension force effects and interface capturing abilities of the VOF method, the well-known 2D dam break case (in OpenFOAM) where water column flows under the effect of gravity is used. The comparison of the water interface location at time t = 0.5 s in Fig. 1 (a) shows good agreement of the hybrid containmentFoam solver with the OpenFOAM inbulit interFoam solver. The minor discrepancies occur in regions with lower volume fractions where the blending function changes the VOF method to mixture method. The validation of the mixture model with drift flux approach for droplets is performed using a 3D bent pipe test case whose geometric details are explained in George et al. [2]. The simulation involves injection of droplets in the main air flow at the inlet of the bent pipe. The droplets while flowing through the bent region of the pipe deviate from the main gas flow path due to their inertia and get deposited on the pipe walls. The droplet inertia increases with diameter and a non-dimensional number Stokes number ($St = \frac{\rho_d d^2 C_c U}{18 \mu_2 R}$) is used to represent different droplet diameters. Here ρ_d is the droplet material density, d is the droplet diameter, C_c is the Cunningham correction factor and R is the radius of the bent pipe. The diameter values and physical properties can be found in George et al. [2]. The volume fraction of droplets on the wall at Stokes number = 0.44 (Fig. 1 (b)) indicates the deposition of the droplets near the bend due to their slip velocity wrt. to the gas flow. The comparison of simulation deposition efficiency ($\eta = \frac{\dot{m}_{deposit}}{\dot{m}_{inlet}}$) for different droplet Stokes numbers with experimental [12], analytical [13] and numerical [14] data demostrated excellent agreement for the Stokes drift model and reasonable agreement for the Maninnen model.

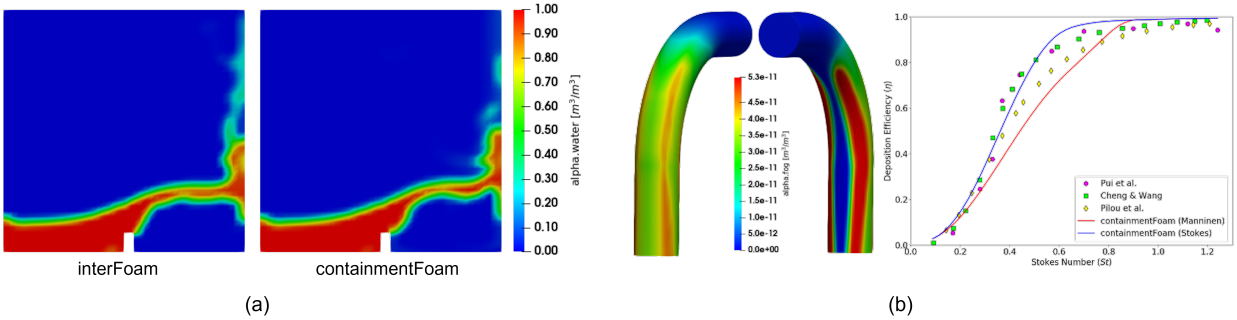

Figure 1. (a): Contours of water interface captured by interFoam compared with containmentFoam for a damBreak case at t = 0.5 s. (b) Left: Deposited droplet volume fraction distribution of the bent pipe wall at Stokes number = 0.44. Right: Experiment vs containmentFoam simulation comparison of inertial deposition efficiency as a function of Stokes number in a bent pipe

3.2. Wall condensation validation test cases

3.2.1. SETCOM facility

The SETCOM (Separate Effects Tests for Condensation Modelling) facility at Forschungszentrum Jülich is designed to provide experimental data for wall condensation studies. The experimental section is a 6 m long flow channel with 0.44 m X 0.44 m cross-section area with a cooled wall where condensation occurs, and the other three walls are insulated [15]. Air-steam mixture is injected at the inlet at different volume fractions, flow velocities and temperature and total wall heat flux along the condensing wall is measured. The experimental setup can be oriented at different inclination angles between horizontal and vertical positions. In the present work, we consider two cases, one in forced convection regime (C035) and another in mixed convection regime (D096). In both cases, the experimental setup is vertical oriented allowing easy flow of condensate downstream under gravity. For validation simulations, a two-dimensional computational domain as shown in Fig. 2 is used and four different meshes with $y^+ \approx 1, 25, 45$ and 75 were used for mesh independency and wall function effect studies for the C035 case. For D096 case, only mesh with $y^+ \approx 1$ is used. The boundary conditions for the simulations are defined in Table. I. Simulations are run by considering both wall and bulk condensation to study the combined effects. The total wall heat flux on the condensing wall is computed by adding the convective heat fluxes by the gas and water phases and, the latent wall heat flux directly added on the wall in film free area of the wall.

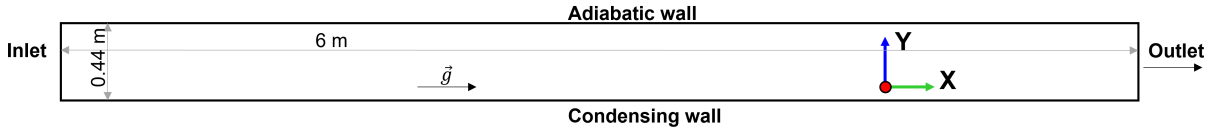

Figure 2. SETCOM two-dimensional computational domain

Table I. Simulation parameters for C035 and D096 test cases

	Forced Convection (C035)	Mixed convection (D096)
Inlet Velocity $[m/s]$	4.2	0.8
Inlet Temperature $[^oC]$	80	80
Condensing wall Temperature $[^oC]$	9	11
Steam volume fraction $[\%]$	30	30
Pressure $[bar]$	1.013	1.013

The results are evaluated after achieving steady state to compare with experimental data. The total wall heat flux along the condensing wall for both test cases (Fig. 3) indicates that the condensation model was able to predict the wall heat flux with good accuracy for both convection regime cases. Even though the $y^+ = 1$ mesh predicted the values for C035 case closer to the experiment, the coarser meshes with wall functions were able to simulate the same with error less than 10 %. This is important from a computational point of view as it can generate reasonably accurate results with less computational power (coarse meshes). The comparison between the single-phase and two-phase results indicated better prediction by the two-phase approach. This is because the single-phase model does not consider the presence of condensed water on the wall which can resist further condensation. Hence, the single-phase model over-predicts condensation and thereby increases total wall heat flux. One of the major improvements achieved by using the two-phase model is to include the effects of presence of condensed water in the system. Although, this

comes at the expense of computational power (30% increase), it offers the benefit of capturing extra features which are not possible in a single-phase framework. Bulk condensation constitutes only 2% of the overall condensation and therefore, it effects on the results are marginal compared to wall condensation. The fog droplets formed due to bulk condensation can be transported by diffusion, convection, and drift. Diffusion of droplets transports it towards the wall where they may get deposited and, also away from the wall where they may evaporate. Also, the droplet drift is primarily due to gravity which is in vertical direction enabling the droplet to leave through the outlet rather than settling on the wall. For the SETCOM cases simulated here, the diffusive and drift transports are marginal compared convective transport due to substantial flow velocity. Hence, the droplet diameter considered for these simulations does not have any notable effect on the results. This was confirmed by running the simulations with two different droplet diameters of $1\mu m$ to $100\mu m$.

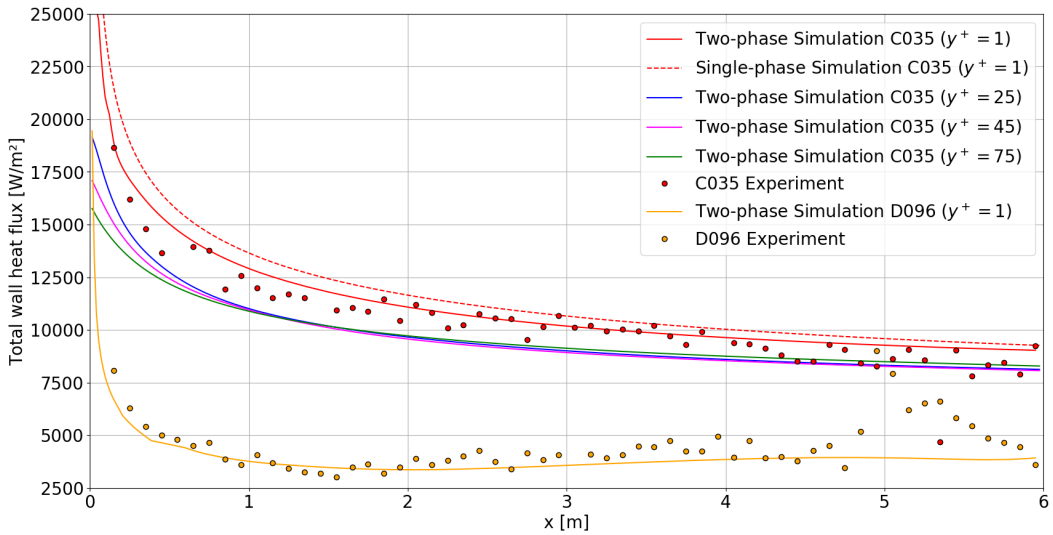

Figure 3. Evolution of wall heat flux along the condensing wall for SETCOM - C035 and D096

3.2.2. COPAIN facility

The COPAIN facility [16] is another experiment like SETCOM operated to study wall condensation. The test section comprises a 2 m long vertically oriented channel (0.6 m X 0.5 m) and the condensing wall (2 m X 0.6 m) is maintained at a low temperature using a coolant circuit. Three different experiments were selected for numerical validation, each corresponding to different convection heat transfer regimes (forced, mixed and natural). A two-dimensional computational domain similiar to Mimouni et al. [4] was chosen for simulation and total wall heat flux along the condensing wall was compared with experimental data. The input parameters for the selected simulations are shown in Table. II. A fine mesh with $y^+ \approx 1$ is used for all simulations and bulk condensation is also considered to investigate its impact.

Fig. 4 compares the total wall heat flux obtained from the simulations with experiments. The natural (P0344) and mixed (P0443) convection cases show excellent agreement with the measured data. However, the forced (P0441) convection simulation over-predicted wall heat flux by around 15 %. This deviation was observed also in the condensation studies by Mimouni et al. [4] and Bucci [17]. They suggested that the model tends to over-predict condensation rate for low Richardson numbers which is the case of forced convection simulation. Also, prediction accuracy within 15 % is acceptable considering experimental uncertainty. Similar to SETCOM, wall condensation is dominant, and the effect of bulk condensation is negligible for

Table II. Simulation parameters for COPAIN validation studies

	P0441 (Forced)	P0443 (Mixed)	P0344 (Natural)
Inlet Velocity $[m/s]$	3	1	0.3
Inlet Temperature $[K]$	353.23	352.33	344.03
Cooled wall Temperature $[K]$	307.4	300.06	322
Air mass fraction $[\%]$	76.7	77.2	86.4
Pressure $[bar]$	1.02	1.02	1.21

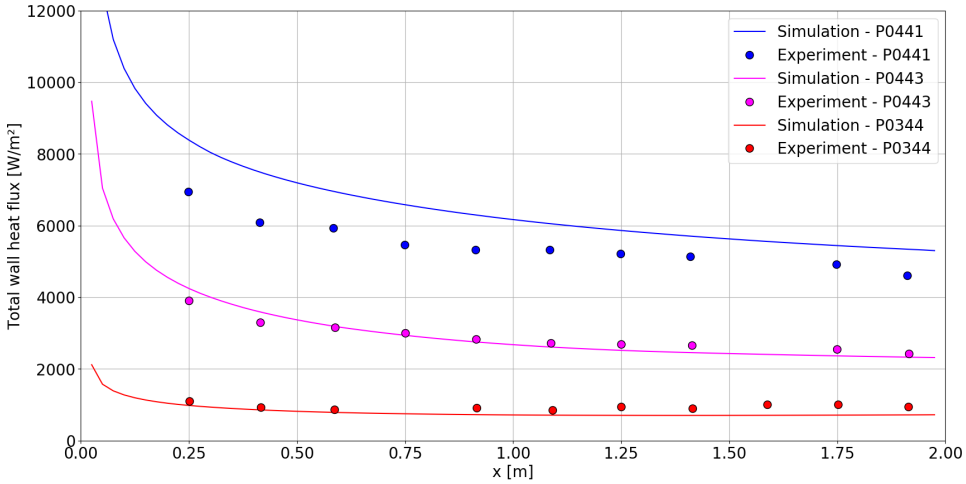

Figure 4. Total wall heat flux distribution along condensing wall for COPAIN - P0344, P0441 and P0443

COPAIN. Also, convective transport of fog droplets is dominant over diffusion and drift which makes the results independent of droplet diameter.

3.3. Bulk condensation verification - Mollier diagram test case

Due to the lack of separate effect studies on bulk condensation, the verification of the bulk condensation model is performed using Mollier diagram theory [18] like Zhang and Laurein [3] and George et al. [2]. Mollier diagram is used to graphically represent the state of an air-steam mixture and state changes during mixing or heat transfer processes. The saturation line which limits the amount steam in air (relative humidity = 100 %) and further addition of steam to air will only result in condensation and mist formation. When two air-steam mixtures at different states (hot and cold) are mixed, the mixing point can be identified using Mollier diagram (or psychrometric chart). However, when the mixing point is below the saturation line, excess steam will condense into fog droplets releasing latent heat, so that the mixture moves to saturation condition. Hence, using Mollier diagram, we can predict the amount of fog formed, mixture temperature and vapor content. Similarly, bulk evaporation can also be verified by mixing a hot and cold air-steam-fog mixture. To simulate the mixing phenomenon, a 2D mixing nozzle geometry [2, 3] with two inlets (0.1 m wide), one outlet and long (5 m) enough to ensure complete mixing is chosen. The inlet conditions of the hot and cold mixtures for both condensation and evaporation simulations are taken from George et al. [2]. Both mixtures were injected at a flow velocity of 1 m/s through the inlets. Since this is a separate effect study,

only bulk condensation model was considered, and wall condensation was deactivated for the simulation runs. Droplet diameter is not relevant here because the Brownian diffusion and slip velocity were ignored.

The simulations generated contours like George et al. [2] which indicated that phase change happens predominantly in the upper part of nozzle and gradually decreases to zero towards downstream as the flows are completely mixed and saturated. The fluid characteristics at the outlet of the nozzle were measured and compared with theoretical values obtained from the Mollier diagram in Table. III. The two-phase bulk condensation model predicted the mixture temperature, vapor, and fog content accurately within 3 % demonstrating good model agreement with theory.

Table III. Comparison of the mixture properties at the nozzle outlet from simulation with Mollier diagram

	Condensation case			Evaporation case		
	Diagram	Model	Error(%)	Diagram	Model	Error(%)
Mixture Temperature $[^oC]$	9.5	9.33	1.84	17	17.14	0.81
Steam content $[g/kg]$	7.4	7.47	0.97	12.2	12.19	0.01
Fog content $[g/kg]$	1.1	1.103	0.25	0.4	0.41	2.5

3.4. THAI TH2 experiment

The ThAI TH2 experiment [19] is a closed cylindrical vessel (60 m^3, internal diameter of 3.2 m, total height of 9.4 m) into which hot steam is injected through a toroidal feed pipe in the upper section. This is a multi-phenomena interaction case where both bulk and wall condensations are important and simulations are performed to find improvements or additional features that can be captured by the two-phase model compared to the single-phase model. Following the previous studies [2, 20, 21], a simplified 2D-axisymmetric mesh with $y^+ = 1$ is selected to conduct the simulations. The vessel has air-steam mixture at initial temperature of 24 ^oC and pressure of 1.042 bar and saturated steam is injected continuously for a period of 2.75 hours. The temperature boundary conditions for the simulations are taken from the transient sensor data of the experiment. In the interest of analysing the fog diameter effect on the results, four different droplet diameters ($d_{fog} = 10\mu m, 25\mu m, 50\mu m$ and $75\mu m$) [3] were selected for the simulations.

The mass transfer rate distribution in the beginning of simulation (Fig. 5(a)) shows that fog formation predominantly takes place near and above the steam feed pipe. There is also some wall condensation happening in the dome of the vessel where the steam hits while traversing upwards under buoyancy effects. Fig. 5(c) shows the fog distribution inside the vessel towards the end of the simulation. It can be observed that, even though the condensation primarily occurs in the upper section, the droplets drift towards the sump of the vessel predominantly under gravity which is demonstrated by higher fog volume fraction in the lower section. Some of these droplets get deposited on the walls and join the wall condensate films which also flows downstream due to gravity. The accumulation of the condensate as water in the sump of the vessel is reflected in Fig. 5(b). The velocity magnitude field in Fig. 5(d) indicates maximum velocity in the injection zone and some moderate velocity the lower portion which is due to the momentum transfer between phases owing to the drifting of fog droplets. Figures 5(e) and 5(f) demonstrate the formation of a stratified layer of steam and temperature inside the vessel at the end of the simulation. However, the temperature layer (Fig. 5(f)) is slightly diffused at the interface which is due to the heat transfer from the fog droplets which drift

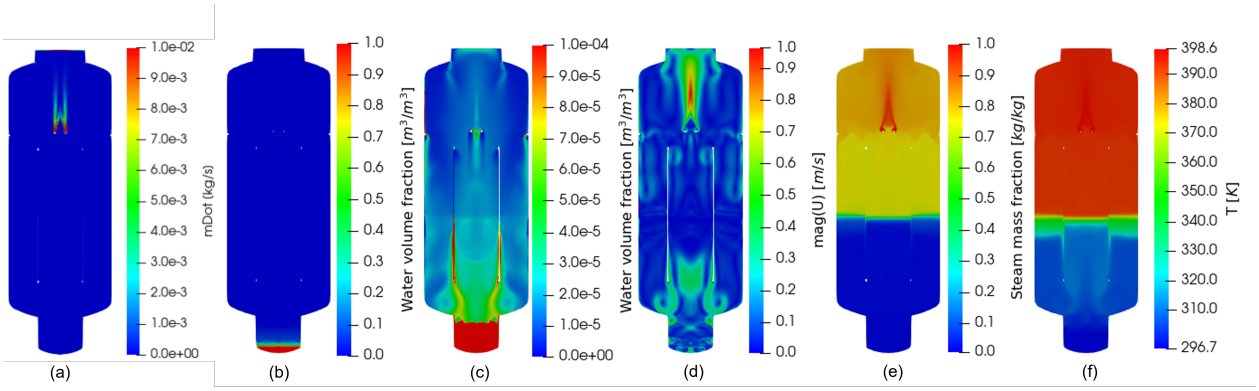

Figure 5. Fields of mass transfer rate (a) at time = 0.27 hours and water volume fraction (b, c), velocity magnitude (d), steam mass fraction (e) and average mixture temperature (f) at time = 2.75 hours for $d_{fog} = 75\mu m$

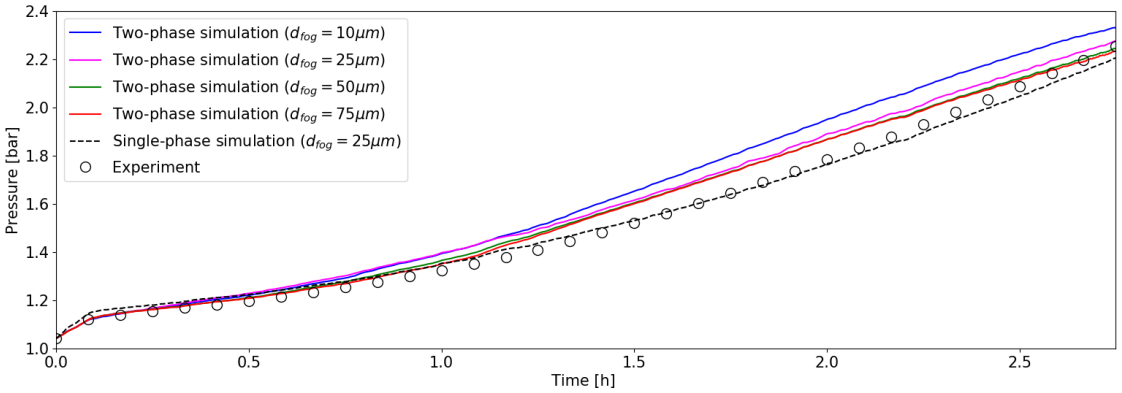

Figure 6. Transient evolution of pressure in the TH2 vessel for single-phase and two-phase (with different droplet diameters) simulations

from the top region (high temperature) to bottom region (low temperature). The transient variation of average pressure inside the vessel with different droplet diameters is compared with single-phase simulation [2] and experimental data in Fig. 6. The two-phase model was able to predict the pressure evolution accurately within 10 % for all droplet diameters. The lowest droplet diameter ($d_{fog} = 10\mu m$) simulation estimated slightly higher pressure compared to other sizes towards the end of the experiment. This is because smaller droplets have lower drift velocities and tend to follow the main flow rather than deviating from it. Hence, they stay suspended in the high temperature upper section where they evaporate as the vessel temperature and pressure increases. However, larger droplets drift downstream to a lower temperature region where they remain as fog and therefore do not contribute to the pressure rise. Another observation from Fig. 6 is that the two-phase simulations over-predict the pressure compared to the single-phase simulations. This is mainly because of the accumulation of water in the sump region which was captured by the two-phase model and was not possible with the single-phase model where the condensate mass is removed from the computational domain. This additional volume occupied by water in the vessel accompanied by some interface evaporation resulted in the over-prediction by two-phase solver. Nevertheless, the two-phase model is closer to the real world and can capture more features than a single-phase model. Also, three-dimensional simulations by including conjugate heat transfer considering the solid vessel walls will be closer to the real experiment and will be pursued in the future.

4. CONCLUSIONS

In this work, we have presented the implementation of two-phase modelling of wall and bulk condensation in *containmentFOAM* CFD package based on OpenFOAM. The solver employs a hybrid VOF-mixture method integrated with drift flux approach in an Eulerian framework to model the transport of water phase constituting dispersed fog droplets as well as continuous water forming gas-water interfaces. The blending function aids in smooth transition from VOF to mixture model based on the local phase volume fraction. The drift flux approach enabled the modelling of the droplet slip velocity considering gravity, drag and inertia effects. The fog formation due to bulk condensation (and evaporation) is modelled by bringing the local mixture to saturation at the simulation time steps by condensing surplus steam and evaporation surplus fog. To simplify the solver, the droplet evolution due to coalescence and break-up was neglected and simulations were performed with constant droplet diameter assumption. The wall condensation is modelled using diffusion layer approach in which rate of condensation is governed by the diffusion of steam towards the wall in the presence of NCGs. Additionally, this model was extended to simulate interface condensation by considering diffusion of steam towards water-gas interface instead of a wall.

The preliminary verification of the ability of the solver to model the peculiar features of VOF and mixture model with dam break and bent pipe deposition case yielded good agreement with previous simulations and experimental data respectively. The wall condensation model was validated using SETCOM and COPAIN experiments, both of which predicted wall flux evolution along the condensing wall with reasonable accuracy. Bulk condensation model verification with Mollier mixing nozzle predicted the outlet temperature and, vapour and fog amount with decent accuracy. Additional validation studies with ThAI TH2 vessel showed that the solver was able to predict the transient evolution of vessel pressure accurately within 15% error. Upcoming works focuses on the implementation of population balance model for incorporating fog droplet evolution mechanisms like coalescence, condensational growth, and fragmentation.

ACKNOWLEDGMENTS

The authors gratefully acknowledge the German Ministry for Economic Affairs and Energy for funding the national THAI-1 project (No. 150 1218) and Becker Technologies (Eschborn, Germany) for carefully documenting and sharing the THAI experimental data. Furthermore, we thank the German Academic Exchange Service (DAAD) for funding the PhD position under the 'DAAD-Research grants for Doctoral Program'.

REFERENCES

1. L. Vyskocil, J. Schmid, and J. Macek, "CFD simulation of air–steam flow with condensation," *Nuclear Engineering and Design*, **279**, pp. 147 – 157 (2014).

2. A. George, S. Kelm, X. Cheng, and H.-J. Allelein, "Efficient CFD modelling of bulk condensation, fog transport and re-evaporation for application to containment scale," *Nuclear Engineering and Design*, **401, 112067** (2023).

3. J. Zhang and E. Laurien, "3D Numerical Simulation of Flow with Volume Condensation in Presence of Non-condensable Gases Inside a PWR Containment," *Proc. W. E. Nagel, D. H. Kröner, M. M. Resch (eds.)High Performance Computing in Science and Engineering '14: Transactions of the high performance computing center, stuttgart (HLRS) 2014*, pp. 479 – 497 (2014), Springer.

4. S. Mimouni, A. Foissac, and J. Lavieville, "CFD modelling of wall steam condensation by a two-phase flow approach," *Nuclear Engineering and Design*, **241**, pp. 4445 – 4455 (2011).

5. S. Kelm et al., "The Tailored CFD Package containmentFOAM for Analysis of Containment Atmosphere Mixing, H2/CO Mitigation and Aerosol Transport," *Fluids*, **6, 100** (2021).

6. W. C. Hinds, *Aerosol Technology*, John Wiley & Sons, 2^{nd} edition (1999).

7. E. M. A. Frederix, A. K. Kuczajd, M. Nordlundd, A. E. P. Veldmanc, and B. J. Geurts, "Eulerian modeling of inertial and diffusional aerosol deposition in bentpipes," *Computers and Fluids*, **159**, pp. 217 – 231 (2017).

8. M. Manninen, V. Taivassalo, , and S. Kallio, *On the mixture model for multiphase*, VTT Publications 288, Technical Research Center of Finland (1996).

9. W. Chung and C. Devaud, "Buoyancy-corrected k– models and large eddy simulation applied to a large axisymmetric helium plume," *International Journal for Numerical Methods in Fluids*, **58**, pp. 57 – 89 (2008).

10. A. Dehbi, F. Janasz, and B. Bell, "Prediction of steam condensation in the presence of noncondensable gases using a CFD-based approach," *Nuclear Engineering and Design*, **258**, pp. 199 – 210 (2013).

11. G. V. Kumar, L. M. F. Cammiade, S. Kelm, K. A. Prakash, and W. Rohlfs, "Implementation of a CFD model for wall condensation in the presence of non-condensable gas mixtures," *Applied Thermal Engineering*, **187, 116546** (2021).

12. D. Y. H. Pui, F. Romay-Novas, and B. Y. H. Liu, "Experimental Study of Particle Deposition in Bends of Circular Cross Section," *Aerosol Science and Technology*, **7** (3), pp. 301 – 315 (1987).

13. Y. S. Cheng and C. S. Wang, "Motion of particles in bends of circular pipes," *Atmospheric Environment*, **15** (3), pp. 301 – 306 (1981).

14. M. Pilou, S. Tsangaris, P. Neofytou, C. Housiadas, and Y. Drossinos, "Aerosol Science and Technology Inertial Particle Deposition in a 90° Laminar Flow Bend: An Eulerian Fluid Particle Approach," *Aerosol Science and Technology*, **45** (11), pp. 1376 – 1387 (2011).

15. S. Kelm et al., "Development of a multi-dimensional wall-function approach for wall condensation," *Nuclear Engineering and Design*, **353, 110239** (2019).

16. P. Bazin and P. Castelli, "COPAIN rapport d'essais, CEA/DRN/DTP internal report," *SETEX/LETS/99-85* (1999).

17. M. Bucci, "Experimental and Computational Analysis of Condensation Phenomena for the Thermal-Hydraulic Analysis of LWRs Containments," *Doctoral dissertation, Ph. D. thesis, University of Pisa* (2009).

18. R. Mollier, "Ein neues Diagramm für Dampf-Luft Gemische," *Z. VDI*, **73**, pp. 1009 – 1013 (1929).

19. T. Kanzleiter, "Experimental facility and program for the investigation of open questions on fission product behaviour in the containment (ThAI = Thermal Hydraulics, Aerosols, Iodine)," ThAI-Experiment TH2, Test Report to Reactor Safety Research Project No. 150 1218 (2002).

20. S. Kelm, J. Lehmkuhl, W. Jahn, and H.-J. Allelein, "A comparative assessment of different experiments on buoyancy driven mixing processes by means of CFD," *Annals of Nuclear Energy*, **93**, pp. 50 – 57 (2016).

21. G. V. Kumar, M. Kampili, S. Kelm, K. A. Prakash, and H.-J. Allelein, "CFD modelling of buoyancy driven flows in enclosures with relevance to nuclear reactor safety," *Nuclear Engineering and Design*, **365, 110682** (2020).